Molecular Cell, Vol. 11, 1349–1360, May, 2003, Copyright ©2003 by Cell Press

Modular Architecture of the Bacteriophage T7 Primase Couples RNA Primer Synthesis to DNA Synthesis

Masato Kato, Takuhiro Ito, Gerhard Wagner, Charles C. Richardson, and Tom Ellenberger*
Department of Biological Chemistry and Molecular Pharmacology
Harvard Medical School
Boston, Massachusetts 02115

Summary

DNA primases are template-dependent RNA polymerases that synthesize oligoribonucleotide primers that can be extended by DNA polymerase. The bacterial primases consist of zinc binding and RNA polymerase domains that polymerize ribonucleotides at templating sequences of single-stranded DNA. We report a crystal structure of bacteriophage T7 primase that reveals its two domains and the presence of two Mg^{2+} ions bound to the active site. NMR and biochemical data show that the two domains remain separated until the primase binds to DNA and nucleotide. The zinc binding domain alone can stimulate primer extension by T7 DNA polymerase. These findings suggest that the zinc binding domain couples primer synthesis with primer utilization by securing the DNA template in the primase active site and then delivering the primed DNA template to DNA polymerase. The modular architecture of the primase and a similar mechanism of priming DNA synthesis are likely to apply broadly to prokaryotic primases.

Introduction

DNA polymerases cannot begin DNA synthesis on single-stranded templates without a primer strand complementary to the template. Conserved residues of DNA polymerase contact the primer strand to align its 3′-hydroxyl for the condensation of nucleotides (Brautigam and Steitz, 1998; Doublie and Ellenberger, 1998). DNA primases synthesize short oligoribonucleotides that are recognized and extended by DNA polymerase (Frick and Richardson, 2001). This priming reaction is repeated frequently on the lagging strand of a replication fork to produce Okazaki fragments during semiconservative replication. During DNA replication, the primase gains access to the lagging strand template through the action of a DNA helicase. In several replication systems, the primase and helicase physically interact (Bird et al., 2000; Chang and Marians, 2000; Marintcheva and Weller, 2001; Valentine et al., 2001). Primer synthesis is also stimulated by interactions with other replication proteins (Benkovic et al., 2001; von Hippel and Jing, 2000; Yuzhakov et al., 1999), and these interactions compensate for the weak template binding of primases and regulate primer synthesis.

The amino acid sequences of primases can be grouped into two families—the prokaryotic primases and the eukaryotic/archaeal primases. Their sequences are unrelated (Griep, 1995; Ilyina et al., 1992) and they have different protein folds (Augustin et al., 2001; Keck and Berger, 2001; Keck et al., 2000; Podobnik et al., 2000). The marked divergence of bacterial and eukaryotic primases makes the bacterial primases attractive targets for selective antibacterial therapeutics. Bacterial primases have six conserved sequence motifs (Ilyina et al., 1992). Motif I residues ligate a zinc metal in the N-terminal zinc binding domain (ZBD), whereas the other conserved motifs (II–VI) are located in the C-terminal RNA polymerase domain (RPD). The ZBD is an important determinant for specific binding to a DNA template (Kusakabe and Richardson, 1996), and it is essential for the synthesis of RNA and the priming of DNA synthesis (Bernstein and Richardson, 1988; Kusakabe et al., 1999; Powers and Griep, 1999). A crystal structure of the ZBD from the *Bacillus stearothermophilus* primase revealed it is a zinc ribbon, a motif present in a variety of DNA and RNA binding proteins (Pan and Wigley, 2000).

The topoisomerase-primase (TOPRIM) fold is a conserved structural motif within the active site regions of the bacterial primases, type IA and type II topoisomerases, and several other phosphoryl transfer enzymes (Aravind et al., 1998). The weakly conserved signature sequence of the TOPRIM fold is present in a number of enzymes catalyzing the metal-assisted formation or cleavage of phosphodiester bonds in DNA (http://pfam.wustl.edu/cgi-bin/getdesc?name=Toprim). Conserved acidic residues of the TOPRIM motif were suggested as metal chelating residues in the active sites of these enzymes. Two crystal structures of the RPD of *E. coli* DnaG primase showed these acidic residues are located in a shallow cleft adjacent to the TOPRIM fold and flanked by primase motifs II–IV (Keck et al., 2000; Podobnik et al., 2000). This cluster of conserved residues, which bound to a Yttrium (Y^{2+}) heavy metal in the crystal structure, was suggested as the location of the primase active site. The TOPRIM folds of DnaG and the topoisomerases are similar, but they are embedded in different structural contexts (Berger et al., 1996; Lima et al., 1994; Mondragon and DiGate, 1999; Nichols et al., 1999), reflecting the different substrate binding requirements and catalytic mechanisms of these enzymes.

Phage T7 encodes DNA polymerase, primase, helicase, and single-stranded DNA binding activities. Together with the *E. coli* thioredoxin, the processivity factor for T7 DNA polymerase, these proteins catalyze the replication of double-stranded DNA (Richardson, 1983). Primase and helicase activities reside in a bifunctional primase-helicase protein that assembles into ring-shaped hexamers having distinctive primase and helicase domains (Egelman et al., 1995; VanLoock et al., 2001) that can be separated by limited proteolysis (Bird et al., 1997; Rosenberg et al., 1996). The C-terminal helicase fragment assembles into a hexameric ring-shaped structure (Guo et al., 1999; Singleton et al., 2000) that translocates 5′ to 3′ along one DNA strand, displacing the complementary strand in a reaction powered by nucleotide hydrolysis (Bird et al., 1997; Matson et al., 1983; Patel et

*Correspondence: tome@hms.harvard.edu

al., 1992). A plausible mechanism of DNA unwinding has been proposed on the basis of crystal structures of helicase fragments (Sawaya et al., 1999; Singleton et al., 2000).

The N-terminal primase of the T7 primase-helicase initiates primer synthesis at the sequence 5′-GTC-3′, templating the synthesis of pppAC. The conserved 3′ C of the priming site is required for RNA synthesis, but it is not copied into the RNA product (Tabor and Richardson, 1981). Functional tetraribonucleotide primers are synthesized at the extended sequence 5′-(G/T)(G/T)GTC-3′, which directs the synthesis of pppACCC, pppACCA, and pppACAC (Frick and Richardson, 1999; Fujiyama et al., 1981; Mendelman and Richardson, 1991). Other bacterial primases recognize different priming sites (Kusakabe et al., 1999; Kusakabe and Richardson, 1996).

T7 primase has two functions during replication. The primase synthesizes oligoribonucleotides for extension by DNA polymerase (Frick and Richardson, 2001). However, the short RNA primers synthesized by T7 primase are not effectively utilized by T7 DNA polymerase unless the primase is present (Kusakabe and Richardson, 1997). Thus, the primase is also necessary for the utilization of primers by DNA polymerase. The primase could stimulate primer utilization by preventing the dissociation of short RNA primers from the DNA template (Kusakabe and Richardson, 1997) or by directly interacting with T7 DNA polymerase to secure the primed DNA template in the polymerase active site (Chowdhury et al., 2000; Kato et al., 2001).

Here, we report crystallographic and NMR studies of an N-terminal fragment of the T7 primase-helicase that encompasses the functional primase. This is the first complete structure of a DnaG-type primase that is fully active in primer synthesis. Together with NMR and biochemical data, the structure reveals that the ZBD and RPD of the primase are brought together during RNA synthesis, and then the ZBD alone delivers the primed DNA template to DNA polymerase.

Results and Discussion

A Fragment of T7 Primase-Helicase Primes DNA Synthesis

An N-terminal fragment (residues 1–272) of T7 primase-helicase that encompasses all six conserved primase motifs synthesizes oligoribonucleotides as efficiently as the intact primase-helicase (Frick et al., 1998). However, the resulting oligonucleotides are not extended by T7 DNA polymerase in the presence of this primase fragment. Since the fragment, lacking a helicase domain, binds to DNA weakly (Frick and Richardson, 1999), we repeated this experiment with a higher concentration of a fragment that was shorter (residues 1–255) and amenable to crystallization. At high concentrations, the fragment can prime DNA synthesis catalyzed by T7 DNA polymerase, albeit less efficiently than the wild-type primase helicase (see Supplemental Data at http://www.molecule.org/cgi/content/full/11/5/1349/DC1). Without the helicase domain, the primase fragment must locate priming sites by random collisions. Nonetheless, all of the essential activities for primer synthesis and primer utilization are present in the 1–255 primase fragment.

Bipartite Structure of T7 Primase

A crystal structure of T7 primase was determined at 2.9 Å resolution (Table 1). The experimental electron density revealed most residues of two primase molecules in an asymmetric unit, with the exception of nine N-terminal residues and a connecting loop between β5 and α1 which are disordered (Figures 1B and 2). Although the crystals are grown in the presence of 2.5 mM ATP and soaked in 20 mM ATP during harvest, there is no electron density for a bound ATP. However, the electron density revealed two metals bound in the active site (Figure 2) and an additional zinc metal that is coordinated by the conserved cysteines of the ZBD.

T7 primase consists of two domains (Figure 1A), a small N-terminal ZBD (residues 10–56) and a larger C-terminal RPD (residues 68–255). An extended polypeptide linker (residues 57–67) connects the ZBD and RPD. Its flexibility is evident from their different orientations in the two primase molecules that were crystallized. After superimposing their RPDs, a rotation of about 30° around an axis of helix α1 is required to superimpose the ZBDs. This flexible connection is notable because it could provide a conditional switch for primer synthesis, bringing together both domains once the primase engages a DNA template. In the hexameric primase-helicase, the flexible connection might allow interactions between adjacent primase domains (Lee and Richardson, 2002). During T7 phage growth, an N-terminally truncated protein lacking the ZBD and the linker of the primase-helicase is expressed by translation initiating from codon 64 (M64) (Dunn and Studier, 1983). This truncated protein has the normal helicase activity, but it is defective in primer synthesis (Bernstein and Richardson, 1988) because it is precisely deleted for the ZBD and the interdomain linker (Figure 4).

The Zinc-Binding Domain

The ZBD of T7 primase is a four-stranded, antiparallel β sheet flanked by a C-terminal α helix (Figure 1A). Its architecture is characteristic of the zinc-ribbon family of metal binding motifs (Qian et al., 1993), and it closely resembles the zinc-ribbon motif from the ZBD of the *B. stearothermophilus* (*Bst*) primase (Pan and Wigley, 2000) (Figure 3; rmsd of 1.1 Å for 23 Cα atoms of these ZBDs). The zinc ribbon of the *Bst* primase has an additional β strand at its N terminus, corresponding to the disordered residues 1–9 of T7 primase. The ZBD interacts with the DNA template during primer synthesis (Bernstein and Richardson, 1988; Kusakabe et al., 1999), and this interaction could organize the N-terminal residues to form the missing β strand. The *Bst* ZBD also has several additional α helices appended to the N- and C-terminal ends, creating a significantly larger structure than the T7 ZBD (Figure 3). An alignment of the sequences of prokaryotic primases reveals gaps at the locations of these additional helices within the ZBD (Figure 4), suggesting that the bacterial primases resemble the larger *Bst* ZBD, whereas the smaller T7 ZBD is emblematic of phage-type primases.

T7 primase binds one atom of zinc (Mendelman et al., 1994), and a bound zinc is evident in the ZBD of both of the primase molecules, based on an anomalous Fourier

Table 1. X-Ray Data and Refinement Statistics

X-Ray Intensity Data	Native[a]	Se-Edge[b]	Se-Peak[b]	Se-Remote[b]	Se-CuKα
Wavelength (Å)	0.9474	0.9797	0.9795	0.9300	1.5418
Resolution (Å)	2.6	2.7	2.7	2.7	2.7
Completeness[c] (%)	98.6 (93.6)	99.9 (99.4)	100 (100)	99.8 (99.6)	97.6 (85.3)
I/σ	14.7	15.2	14.2	19.1	17.1
R_{sym}[c,d] (%)	5.6 (24.1)	7.3 (32.2)	8.1 (38.8)	6.6 (21.8)	8.0 (39.8)
Phasing power		1.64	1.17	0.88	0.59
CullisR (a/c)[e] (%)		−/−	0.82/0.74	0.79/0.69	0.86/0.78
CullisR (ano)[f] (%)		0.60	0.59	0.68	0.89
Figure of merit[c] (15-2.7 Å)	0.60 (0.38)				
Refinement statistics					
Resolution (Å)	10-2.9				
R_{cryst}/R_{free}[g] (%)	23.4/27.6				
Rms deviations					
Bond length (Å)	0.008				
Bond angles (°)	1.46				
Torsion angles (°)	1.18				
Overall mean B value (Å^2)	19.9				
Number of atoms					
Protein	3763				
Water	14				
Metal ions	6				
Ramachandran plot					
Most favored (%)	79.4				
Allowed (%)	19.9				
Generously allowed (%)	0.7				

[a] Collected at the station F1 of the Cornell High Energy Synchrotron Source (Ithaca, NY).
[b] Collected at the beamline X8C of the National Synchrotron Light Source (Upton, NY).
[c] The numbers in brackets represent the values for the last resolution shells.
[d] $R_{sym} = \Sigma_{hkl} \Sigma_i | I(hkl)_i - \langle I(hkl) \rangle | / \Sigma_{hkl} \Sigma_i \langle I(hkl)_i \rangle$.
[e] a and c indicate acentric and centric reflections, respectively.
[f] ano, based on anomalous diffraction differences.
[g] R_{free} was calculated using 5% of the reflection data.

map calculated with X-ray data collected at the K absorption edge for zinc (λ = 1.284 Å). The zinc atom is coordinated in a tetrahedral geometry by two pairs of cysteine residues located in the β2/β3 loops and the β4/β5 loop of the ZBD. A similar geometry of zinc coordination was reported for the *Bst* ZBD, except that a histidine replaces one of the cysteines (Pan and Wigley, 2000). The zinc binding site of T7 primase is partially exposed on the surface of the ZBD facing away from the active site. Its location and the chemical characteristics of the surrounding residues suggest that the zinc atom does not directly participate in interactions with DNA or with nucleotides. The bound metal is instead likely to support primer synthesis by stabilizing the protein fold of the ZBD. The surface of the ZBD away from the zinc binding site and facing the RPD is likely to interact with the DNA template. A hinge-like motion of the linker could bring the ZBD and RPD together and allow both domains to contact the template during RNA synthesis. The proposed DNA binding surface of the ZBD is decorated with a central patch of aromatic residues (F11, F29, Y37, Y35, and W42) that are surrounded by a rim of polar and charged residues (H14, D24, D31, H33, E40, and K41). Aspartate 31 and H33 are important determinants of binding to the 5′-GTC-3′ priming sites (Kusakabe et al., 1999). In the crystal, two neighboring ZBDs pack against one another and bury the aromatic residues that we propose could stack against the bases of a DNA template.

The RNA Polymerase Domain

The RPD is composed of two substructures, a C-terminal TOPRIM fold that resembles the corresponding region of the *E. coli* DnaG primase (Keck et al., 2000; Podobnik et al., 2000) and a structurally divergent N-terminal subdomain with a mixed α/β fold (Figures 1 and 3). A shallow cleft separates these subdomains, and the residues of conserved motifs II–VI (Figure 4) are clustered near the cleft. The overall shape of the RPD is unlike the cashew-like silhouette of the DnaG RPD (Figure 3A) because of the divergent N-terminal subdomains of these RPDs. DnaG has an additional C-terminal extension that mediates interactions with the DnaB helicase. T7 primase lacks this structure and is covalently joined to the helicase in a bifunctional primase-helicase.

The N-terminal subdomain of the T7 RPD consists of an antiparallel, four-stranded β sheet packed against an α helix and two short 3_{10} helices. Primase motifs II and III are located in the connecting loops between a pair of helices (γ2/α2) and a pair of β strands (β7/β8) within this subdomain. These conserved residues face the shallow cleft separating the N-terminal subdomain from the TOPRIM fold (Figures 1A and 4). DnaG has an analogous four-stranded β sheet but is otherwise dissimilar in the N-terminal subdomain of its RPD (Figure 3). An insertion between strands β1 and β4 of this β sheet significantly increases the overall size of DnaG's RPD (Figure 4). An α helix located at the N terminus of the DnaG RPD (helix α1) replaces part of the extended

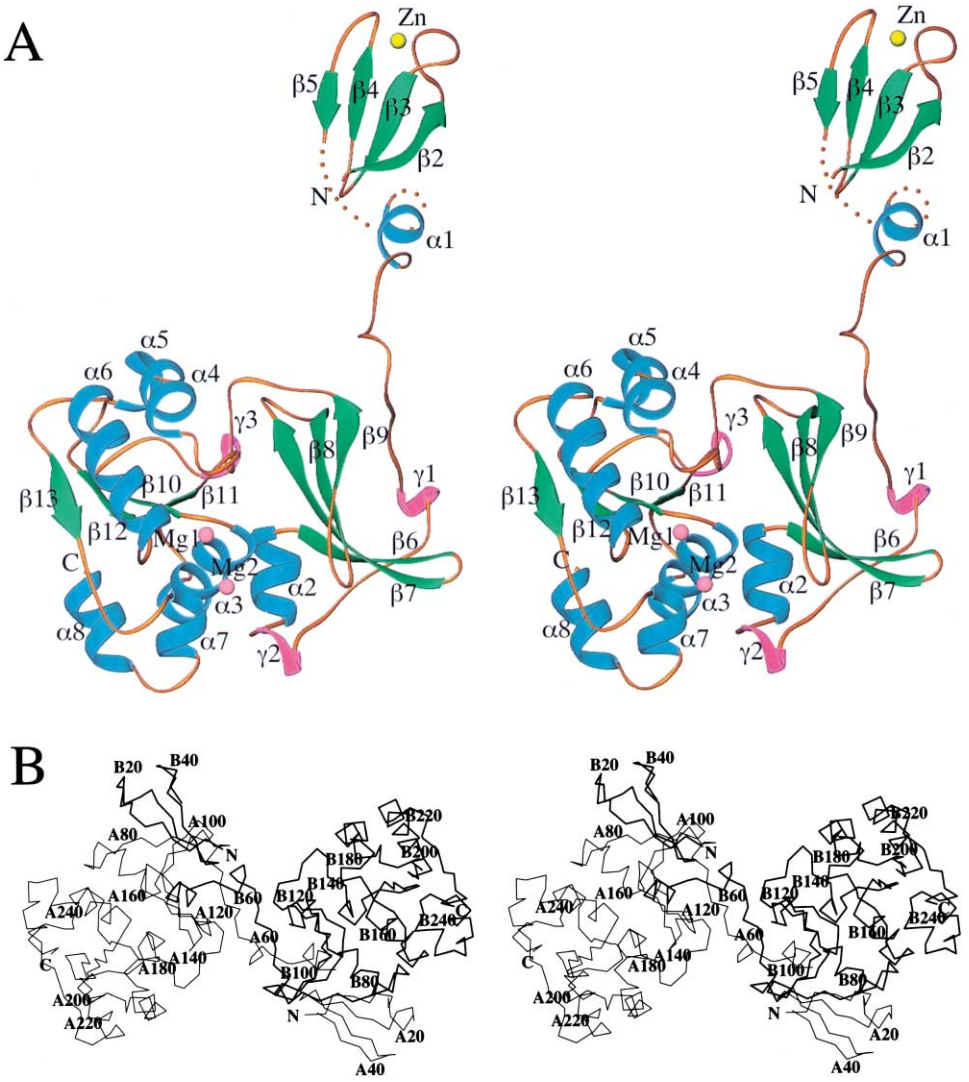

Figure 1. Crystal Structure of T7 Primase

(A) A stereo diagram of T7 primase is shown as a ribbon model with the secondary elements colored; α helix (blue), β strand (green), and 3_{10} helix (magenta). Dotted lines denote disordered regions of the protein (residues 1–9 and 45–48 of the molecule shown here). A zinc atom (yellow) and two magnesium atoms (pink) are bound to the primase.

(B) Two primase molecules that occupy the asymmetric unit of the crystals are related by noncrystallographic 2-fold symmetry, with the ZBD of each molecule "swapped" onto the RPD of the neighboring molecule.

linker that connects the RPD of T7 primase to the ZBD (Figure 3), possibly making this connection more rigid in DnaG.

The TOPRIM Fold and the Primase Active Site

The C-terminal TOPRIM fold of T7 primase consists of a four-stranded β sheet sandwiched between five α helices and a 3_{10} helix (Figures 3 and 4). It contains the residues from conserved motifs IV–VI, and it resembles the TOPRIM fold of DnaG (Figure 3). A search of the Protein Data Bank (Holm and Sander, 1993) revealed that the TOPRIM fold of T7 primase is structurally similar to the TOPRIM folds from a variety of DNA topoisomerases (Rmsd $<$ 3 Å; see Supplemental Data at http://www.molecule.org/cgi/content/full/11/5/1349/DC1) despite the weakly conserved amino acid sequences.

Mutational studies of prokaryote primases have identified catalytically important residues (Lee and Richardson, 2001; Sun et al., 1999; Ziegelin et al., 1995) located around the shallow cleft between the TOPRIM and N-terminal subdomains of the RPD (Figures 1A and 4). Five invariant acidic residues (E157, D161, D207, D209, and D237) from primase motifs IV–VI cluster on the TOPRIM side of the cleft, creating an acidic patch at the center of the active site (Figures 2 and 5D). These residues bind two metal ions in the crystal structure (Figures 1A and 2). We presume these are Mg^{2+} ions because the electron density corresponding to the metals increases after soaking crystals in magnesium concentrations higher than 2.5 mM $MgCl_2$. The side chains of E157 and D207 coordinate one of the metals (Figure 2). The side chain of D209 also points toward the bound

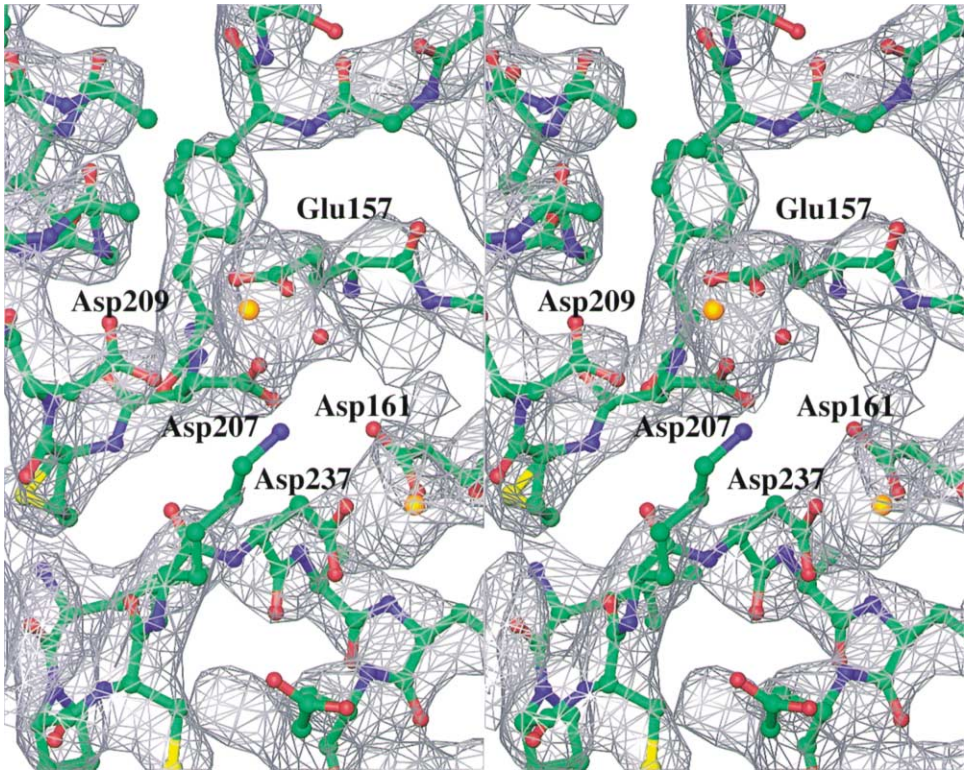

Figure 2. Metal Binding in the Active Site of T7 Primase

A stereo view of the primase active site is shown with the experimentally phased electron density superimposed, contoured at 1 σ. The conserved acidic residues of primase motifs V and VI are labeled and they chelate two Mg^{2+} ions (gold spheres). A nearby water molecule (red sphere) is coordinated by one of the Mg^{2+} ions.

metal, but the distance is too far for a direct contact with the metal. These three acidic residues are perfectly conserved in proteins containing the TOPRIM fold, and their spatial arrangement resembles that of a conserved triad of acidic residues within the active site of RNA polymerases (Gnatt et al., 2001; Vassylyev et al., 2002). This cluster of acidic residues coordinates a Mg^{2+} ion in a crystal structure of topoisomerase IV (Nichols et al., 1999) and a Y^{2+} ion in the structure of the RPD of DnaG (Keck et al., 2000), although this metal binding site in DnaG was not detected by Fe^{2+} affinity cleavage (Godson et al., 2000). A second Mg^{2+} ion is coordinated by D237 of T7 primase (Figure 2), and it corresponds to the metal binding site of DnaG that was detected by Fe^{2+} affinity cleavage (Godson et al., 2000). However, this second metal site was not occupied in crystal structures of DnaG (Keck et al., 2000; Podobnik et al., 2000). Aspartate 237 is a conserved residue of primase motif VI, but it is not conserved in all TOPRIM folds. We are less certain about the biological significance of the second bound Mg^{2+}, but biochemical evidence suggests that DnaG binds at least two Mg^{2+} ions (Urlacher and Griep, 1995). Prima facie, the two Mg^{2+} ions are reminiscent of a two metal-ion mechanism of nucleotide polymerization (Steitz, 1998).

A group of basic residues in the N-terminal half of the RPD faces the shallow cleft between the N-terminal and TOPRIM subdomains of T7 primase. Lysine 122, K128, K131, and K137 all contribute to RNA synthesis activity (Lee and Richardson, 2001). They are in a region corresponding to the ATP binding site of DnaG, which was identified by crosslinking of ATP analogs to K241 (Mustaev and Godson, 1995; Sun et al., 1999), corresponding to K137 of T7 primase. These data implicate the shallow cleft as the binding site for nucleotide.

Interaction with DNA and Nucleotide Substrates

The T7 primase crystallized in an open conformation with its ZBD and RPD some distance apart (Figure 1). These domains must come together to engage nucleotides and the DNA template. The ZBD is directly involved in binding to DNA (Kusakabe et al., 1999; Kusakabe and Richardson, 1996; Mendelman et al., 1994), especially the residues D31 and H33, which recognize the cryptic 3′ C of the priming site. The bacterial primases have an analogous pair of charged residues in the β3/4 loop (E55 and K56 of the *Bst* ZBD) (Pan and Wigley, 2000), suggestive of a similar mode of interaction with their DNA templates. A simple, hinge-like bending of the flexible linker between the ZBD and RPD could bring D31 and H33 closer to the primase active site to help position the DNA template for interactions with nucleotides (Figure 5D). The ZBDs of two primase molecules are intertwined so that the ZBD of each molecule packs against the adjacent RPD in a domain swapping arrangement (Figure 2B) that we believe has no biological significance. These crystal-packing interactions would appear to prevent movement of the ZBD in response to sub-

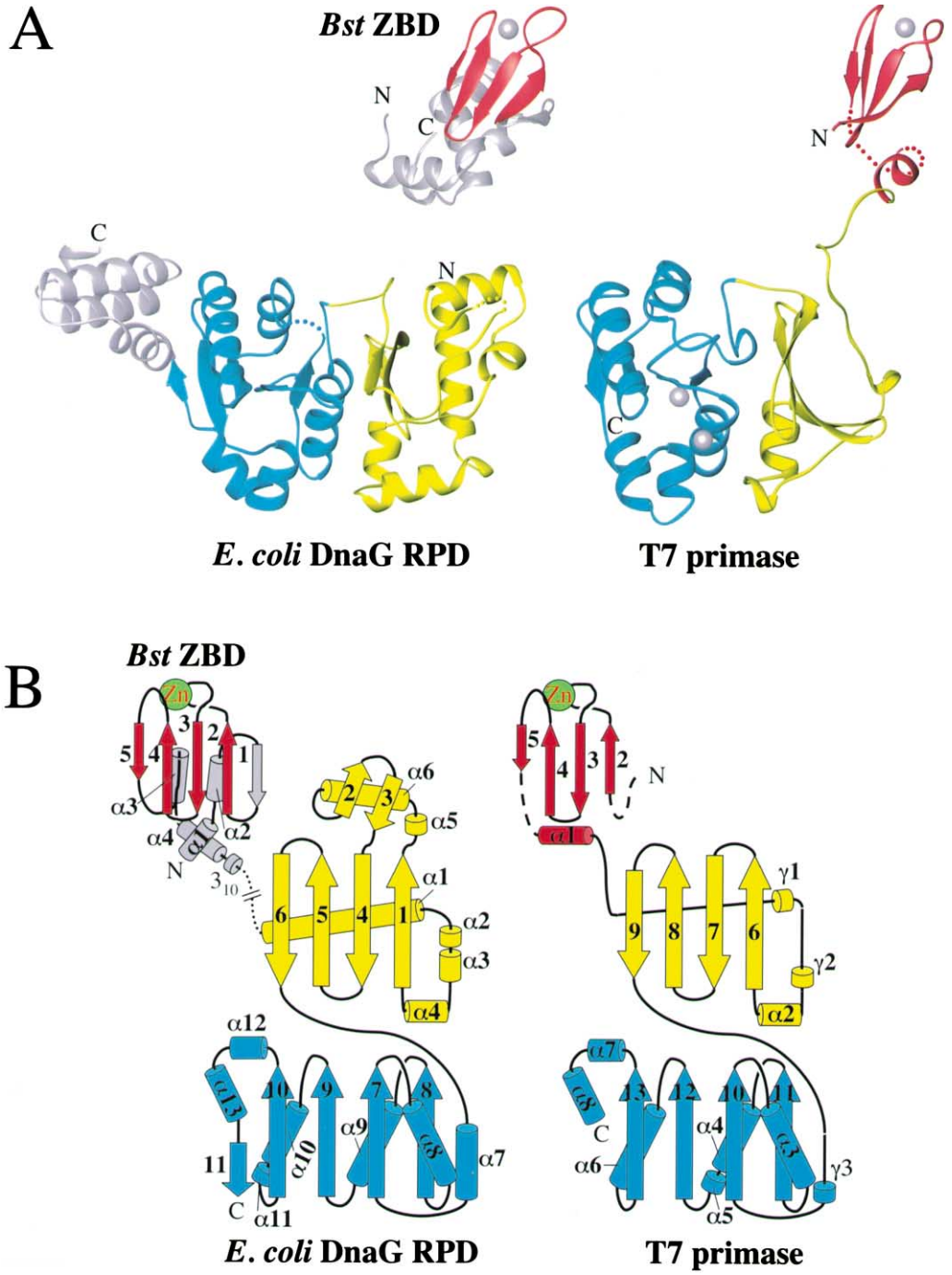

Figure 3. Modular Architecture of T7 and DnaG Primases

(A) The structure of T7 primase has features resembling the ZBD of *Bst* primase (Pan and Wigley, 2000) and the RPD from *E. coli* DnaG (Keck et al., 2000; Podobnik et al., 2000). The structurally conserved regions are colored as follows: the zinc ribbon motif (red), the N-terminal subdomain of the RPD (yellow), and the C-terminal TOPRIM fold (blue). The bound metal ions in T7 primase are depicted as silver spheres. *Bst* ZBD has additional α helices (gray) flanking the conserved zinc ribbon motif. A unique subdomain at the C terminus of DnaG (gray) supports its interactions with the DnaB helicase.

(B) A topological comparison of the primases. The subdomains are colored as (A), and the secondary structures are depicted as arrows for β strands and cylinders for α helices and 3_{10} helices. The broken lines indicate disordered regions of T7 primase. The dotted line between *Bst* ZBD and the RPD of *E. coli* DnaG indicates the predicted connection between these domains.

strates. We therefore examined the interaction of T7 primase with a DNA template and an oligoribonucleotide primer using nuclear magnetic resonance.

In the absence of ligands, the ^{1}H-^{15}N HSQC spectrum of T7 primase shows a number of well-resolved amide N-H cross peaks characteristic of a folded protein along

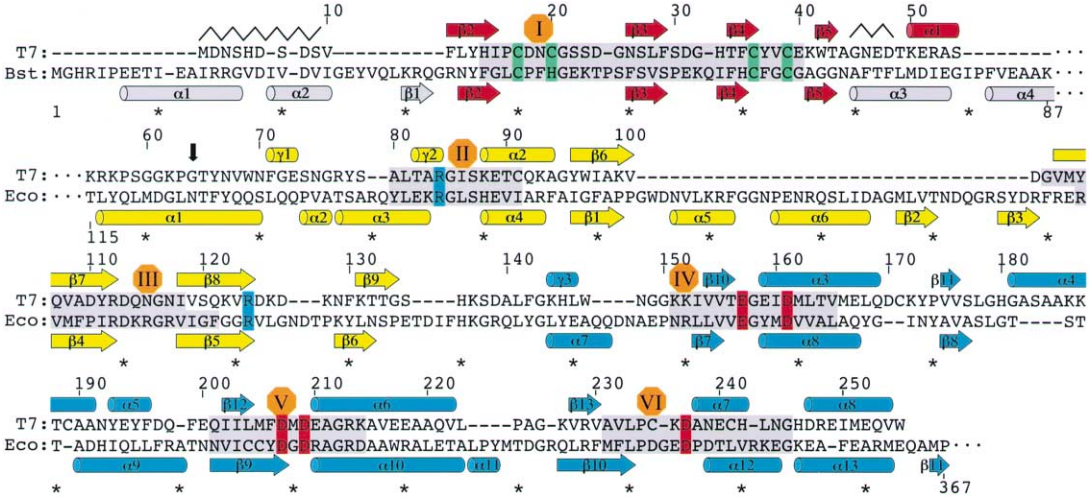

Figure 4. Structure-Based Sequence Alignment of T7 Primase with Bacterial Primases

Structures of the ZBD of the *Bst* primase (Pan and Wigley, 2000) and the RPD of *E. coli* DnaG (Keck et al., 2000) were superimposed on T7 primase, and the structurally aligned amino acids are shown here. The secondary structures of these proteins are indicated above and below each sequence as cylinders (α helices), arrows (β strands), or cylinders labeled "γ" (3_{10} helices). The wavy lines show residues that are disordered in the crystal structures. The conserved primase motifs defined by Ilyina et al. (1992; colored gray) include five highly conserved acidic residues (red) and two arginines (blue). The black arrow indicates the starting residue of a truncated form of T7 primase-helicase that is expressed with the full-length protein during phage growth.

with unresolved peaks at the crowded center region of the spectrum (Figure 5A). A closer inspection of the HSQC spectrum reveals a distinct class of well-dispersed proton resonances with higher-than-average intensities. These stronger peaks probably correspond to residues from the smaller ZBD, moving independently and with a shorter correlation time than the larger RPD and thus generating narrower and taller signals. The ^{1}H-^{15}N HSQC spectrum of the ZBD alone was also recorded, and it confirms that the well-dispersed peaks arise from amide protons of residues within the ZBD (compare Figures 5A and 5C). The conservation of the peak positions of the ZBD in full-length primase indicates that the ZBD doesn't tightly associate with the RPD. Additional evidence supporting this conclusion is obtained from ^{15}N relaxation experiments. The T_1 and T_2 relaxation times of residues from the ZBD and RPD of the primase fall into two distinctly different groups that indicate that the ZBD exhibits significantly faster rotatory diffusive motion than the RPD (see Supplemental Data at http://www.molecule.org/cgi/content/full/11/5/1349/DC1). We conclude that in the absence of substrates the ZBD and RPD move independently and there is little interaction between these domains.

Upon addition of a DNA template and a complementary oligoribonucleotide primer (5′-ACCC-3′), the ^{1}H-^{15}N HSQC spectrum of T7 primase changes dramatically with the well-dispersed resonances from the ZBD shifting position or disappearing altogether (compare circled peaks in Figures 5A and 5B). A number of unassigned peaks also change in response to substrate binding, including many residues that are most likely from the RPD (peaks not circled in Figures 5A and 5B). The observed spectral changes arising from residues in both the ZBD and RPD indicate that both domains interact with the primed DNA template, consistent with the model shown in Figure 5D. However, the spectrum of Figure 5B has less than the expected number of peaks, indicating that part of the system is not in a unique state but fluctuates between different conformations leading to broadening of peaks. The disappearance of signals could also be due to aggregation. However, a large fraction of the signals originating from the RPD remains unchanged (Figure 5B versus 5A), indicating there is no major problem with aggregation of the system. In addition, Figures 5A and 5B show a region of poorly structured signals in the center of the spectrum. This is often observed in proteins that are partially aggregated or contain unstructured segments. Because this feature of the spectrum is similar before and after the addition of the primed template, we conclude that addition of substrate does not cause additional aggregation of the primase. In contrast to the spectral changes seen in Figure 5B, the HSQC spectrum of the primase does not change upon addition of the DNA template alone. However, the subsequent addition of ATP and CTP to activate RNA synthesis triggers the same spectral changes as those described above. The involvement of both the ZBD and RPD in binding to a primed DNA template could be explained either by closure of the primase in *cis* (Figure 5D) or by the interactions of the ZBD and RPD from two different primase molecules in *trans*. Although the NMR experiments do not distinguish between these possibilities, *trans* interactions between neighboring primase domains of the ring-shaped T7 primase-helicase appear to be unfavored (E. Toth and T.E., unpublished data).

We propose that the ZBD secures the DNA template in *cis* within the active site of the RPD, allowing nucleotides to base pair with the template and contact the metals ligated by residues of primase motifs V and VI (Figure 5D). We have modeled the interaction of the

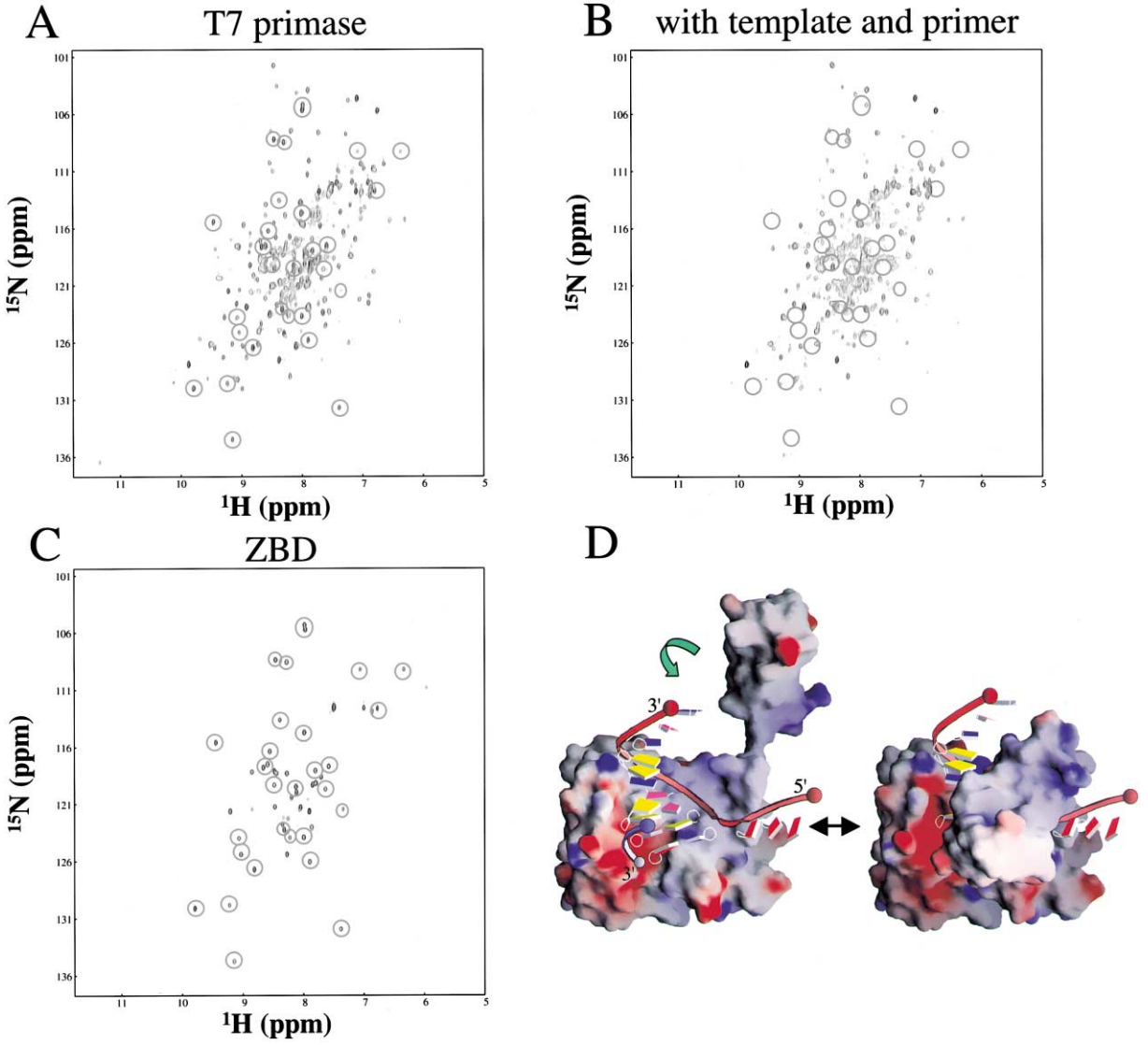

Figure 5. The Conformation of T7 Primase Changes Upon Binding to a Primed DNA Template

(A) A two-dimensional ^{1}H-^{15}N HSQC spectrum of T7 primase is shown. Many of the well-dispersed peaks are from residues within the ZBD (circled; cf. [C]).

(B) The HSQC spectrum of the primase changes dramatically upon binding to a DNA template annealed with the tetraribonucleotide ACCC. The well-dispersed peaks arising from the ZBD (circled, compare with [A]) disappear in complex with the primer-template pair. Many of the unassigned peaks (uncircled) arising from the RPD also change in the complex, indicating that both domains engage the primed template.

(C) The two-dimensional ^{1}H-^{15}N HSQC spectrum of the ZBD alone (residues 1–59) shows the locations of peaks arising from the residues of the ZBD.

(D) The NMR data of (A) through (C) can be explained by a substrate-induced change in the conformation of T7 primase from that seen in the crystal structure of the unliganded primase (see Experimental Procedures for the modeling exercise). In the closed conformation modeled here, the primase engages the primer 3′ end (blue strand) in the RPD active site while the ZBD contacts the priming site of the template (red strand). The solvent accessible surface of the primase is shown, colored according to electrostatic potential (blue $\geq$ $^{+}$12 kT; red $\leq$ $^{-}$12 kT; calculated with GRASP [Nicholls et al., 1991]).

ZBD domain with the bases of the primase recognition sequence 5′-GTC-3′ to include contacts with D31 and H33, important determinants of DNA binding specificity (Kusakabe et al., 1999; Kusakabe and Richardson, 1996). This model places the most highly conserved and the functionally important residues close to the template and/or the bound nucleotides, and the 3′ end of the RNA next to the metal binding sites of the active center. The model also suggests several mechanisms for limiting the length of oligoribonucleotides synthesized by the primase. If the ZBD remains bound to the priming site during nucleotide polymerization, then translocation of the DNA template might be restricted by the length of the ZBD tether. Alternatively, the ZBD might remain docked to the active center as the template translocates during RNA synthesis, causing a progressive loss of sequence-specific DNA interactions that limits product extension. The data presented below suggest that the

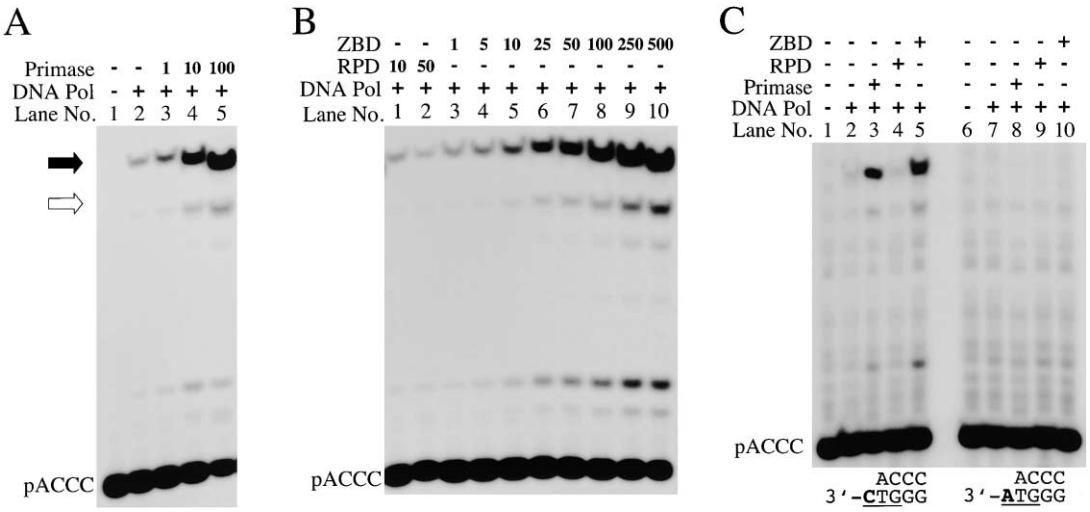

Figure 6. The ZBD of T7 Primase Stimulates Primer Utilization by T7 DNA Polymerase

(A) The efficient extension of oligoribonucleotides by T7 DNA polymerase requires the addition of T7 primase (see Experimental Procedures). Lane 1, no proteins added; lane 2, T7 DNA polymerase (1 μM) only; lanes 3–5, addition of T7 DNA polymerase (1 μM) plus T7 primase at the indicated concentrations (μM). The fully extended primer strand (black arrow) and one of the abortive products (white arrow) are indicated.

(B) Similar reactions were carried out with the RPD or ZBD of the primase added separately. The RPD has no effect on primer utilization, whereas the ZBD stimulates primer extension by T7 DNA polymerase to the same extent as the intact primase. Lanes 1 and 2, T7 DNA polymerase (1 μM) plus the RPD at indicated concentrations (μM); lanes 3–10, the DNA polymerase (1 μM) plus the ZBD at the indicated concentrations (μM).

(C) The cryptic 3′ cytidine of the priming site (underlined) is required for stimulation of DNA synthesis by the primase. Lanes 1–5, reactions templated by the correct 3′-CTGGG-5′ priming site using the combinations of proteins indicated at the top of the figure. Lanes 6–10, similar reactions using the modified priming site, 3′-ATGGG-5′, which anneals to the pACCC primer but lacks the cryptic 3′ C. On the modified template, T7 primase (lane 8) and the ZBD (lane 10) are unable to stimulate primer extension.

ZBD remains bound to DNA during RNA synthesis and in the subsequent step when the primed DNA template is passed to T7 DNA polymerase.

The ZBD Stimulates Primer Utilization by T7 DNA Polymerase

In addition to synthesizing primers, T7 primase also enhances the efficiency with which the primers are extended by T7 DNA polymerase. Given the short length of the primer, we might expect the primase to be intimately associated with T7 DNA polymerase to promote extension of the primer by the polymerase (Chowdhury et al., 2000; Kato et al., 2001). However, our attempts to create a docking model of the primase bound to DNA polymerase were frustrated by the large size of the RPD in comparison to the narrow DNA binding groove of the polymerase. We therefore considered the possibility that the ZBD alone could deliver the primed DNA template to T7 DNA polymerase.

T7 DNA polymerase initiates DNA synthesis efficiently on a template annealed to a tetraribonucleotide (pACCC) only when the primase is present (Figure 6A). The stimulation of primer utilization by T7 DNA polymerase is maximal at micromolar concentrations of T7 primase (see Supplemental Data at http://www.molecule.org/cgi/content/full/11/5/1349/DC1), consistent with its lower DNA binding affinity compared to the full-length primase-helicase (Kato et al., 2001; Kusakabe et al., 1998). The RPD alone (50 μM) does not stimulate the extension of primers by T7 DNA polymerase, whereas the ZBD does support primer extension (Figure 6B), albeit less efficiently than the intact primase. Thus, the ZBD is mainly responsible for enhancing primer utilization and the RPD is not required during primer extension by T7 DNA polymerase. The cryptic 3′ C of the 5′-GTC-3′ recognition sequence is required not only for RNA synthesis (Frick and Richardson, 1999) but also for the utilization of the primer by DNA polymerase (Figure 6C). Since the ZBD specifically interacts with the 3′ C of the priming site (Kusakabe and Richardson, 1996), this result implies that the ZBD remains bound to the primed DNA template as DNA polymerase engages the primer.

The HSQC spectrum of the primase bound to a primed DNA template (Figure 5B) is suggestive of a conformational equilibrium—the peaks are significantly broadened when the primase is complexed to RNA and DNA (compare Figures 5A and 5B). We suggest this equilibrium is populated by the closed primase complex depicted in Figure 5D and an open conformation in which the ZBD remains bound to the primed template. We conclude that the ZBD remains bound to the primed DNA template while RPD is released, exposing the primed DNA template and ZBD of the primase for interactions with DNA polymerase. This interpretation is consistent with modeling studies showing that the RPD is too large to fit into the DNA binding groove of T7 DNA polymerase, whereas the smaller ZBD can be accommodated in complex with a nascent RNA primer that is being extended by the polymerase. A unique loop (residues 401–404) located at the base of the thumb of T7 DNA polymerase is also required for primer utilization (Chowdhury et al., 2000), and this loop might interact with the ZBD at the onset of primer extension.

Conclusions

The crystal structure and NMR studies of T7 primase reveal a flexible linkage between the ZBD and RPD that allows the ZBD to perform two essential functions. The ZBD recognizes the temple sequence for primer synthesis and assists this reaction by securing the template into the active site of the primase. After the primer is synthesized, the ZBD materially participates in primer extension by T7 DNA polymerase. The modular architecture of the primase allows the ZBD to freely dissociate from the RPD to deliver the primed template to the DNA polymerase. The related DnaG primase from *E. coli* transfers its primers to the processivity clamp of DNA polymerase instead (Yuzhakov et al., 1999). Given their functional and structural similarities to T7 primase, it seems likely that other prokaryotic DNA primases could similarly chaperone primed templates to DNA polymerase or its associated factors.

Experimental Procedures

Expression and Purification of T7 Primase Proteins

The coding sequence for the T7 primase fragment (residues 1–255) was amplified by polymerase chain reaction and cloned into the expression plasmid pET17b (Novagen). A bacterial expression plasmid for the ZBD (residues 1–59) was similarly constructed in pET17b. Proteins were expressed in *E. coli* BL21(DE3) cells grown in Luria-Bertani medium at 37°C until the culture reached an $OD_{600} \approx 1.5$. The culture was then chilled to 25°C, and protein expression was induced for an additional 18 hr. The primase was purified as described (Frick et al., 1998), except that the HiTrap blue affinity column was substituted with heparin sepharose. The purified primase was concentrated to 50 mg ml^{-1} by ultrafiltration (Centricon 10; Amicon Inc) and then diluted with an equal volume of glycerol and stored at −20°C. The selenomethionine-substituted primase was overexpressed in M9 minimal media containing 60 mg L^{-1} selenomethionine and 10 μM $ZnSO_4$ as described (Van Duyne et al., 1993) and purified as described above. Perdeuterated-^{15}N-labeled proteins were expressed in M9 minimal media prepared with ^{15}N-$(NH_4)_2SO_4$ and 10 μM $ZnSO_4$ in D_2O. The purification of the ZBD was carried out as described above except that the heparin sepharose chromatography step was omitted. The purified RPD was provided by Luis Brieba (Harvard Medical School).

RNA-Primed DNA Synthesis Assay

The RNA-primed DNA synthesis assay was described previously (Kato et al., 2001), with the following modifications. The reaction mixture (10 μl) contained 40 mM Tris-HCl (pH 7.5), 10 mM $MgCl_2$, 10 mM DTT, 100 μg ml^{-1} BSA, 50 mM potassium glutamate, 25 ng μl^{-1} M13 ssDNA, 1 mM each of ATP and CTP, 0.3 mM each of dATP, dCTP, and dGTP, 0.3 mM [^{3}H]-dTTP, 100 nM T7 DNA polymerase, and the indicated concentrations of gp4 protein, T7 primase, or a monomeric mutant of the gene 4 protein, gp4ΔD2D3 (Kato et al., 2001). The reactions were incubated for 30 min at 37°C, and DNA synthesis was measured using a previously described filter binding assay (Lee et al., 1998). DNA synthesis assays using a synthetic ribotetranucleotide (ACCC) were carried out in reactions containing 100 μM 26-mer DNA template (5′-CAGTGACGGGTCGTTTATCGTC GGCA-3′) and 100 μM [^{32}P]-ACCC instead of M13 ssDNA, ATP, and CTP, and the indicated concentrations of T7 primase, the ZBD, or the RPD. The mixtures were incubated for 1 hr at 25°C. The reactions were quenched with an equal volume 98% formamide containing bromphenol blue, followed by separation of the products on a 25% acrylamide gel containing 3M urea and autoradiography.

X-Ray Structure Determination of T7 Primase

T7 primase was crystallized by the hanging drop vapor diffusion method. The protein drop initially contained 8 mg ml^{-1} primase in 50 mM MES (pH 6.3), 2 M sodium formate, 5.5 mM DTT, and 2.5 mM ATP. The reservoir solution contained 100 mM MES (pH 6.3), 4 M sodium formate, and 5.5 mM DTT. Crystals grew at 22°C over the course of 1 week. The crystals belong to space group $P3_121$ with unit cell dimensions of a = 138.6 Å, b = 138.6 Å, and c = 85.4 Å. There were two molecules of the primase in the asymmetric unit with a solvent content of approximately 67%. The selenomethionine protein crystallized under the same conditions as the wild-type protein.

The structure was determined by a multiwavelength anomalous diffraction experiment using crystals of the selenomethionine-substituted protein (Table 1). The crystals diffract X-rays to a resolution of 2.3 Å in some directions, but the crystallographic model was refined against the isotropic X-ray data extending to a resolution limit of 2.9 Å. The crystals were transferred in the harvest solutions containing 50 mM MES (pH 6.3), 4 M sodium formate, 5 mM DTT, and 5 mM $MgCl_2$ and incubated for 1 hr at 22°C. The concentration of $MgCl_2$ was incrementally adjusted in 5 mM steps to a final concentration of 20 mM. The crystals were then transferred in a cryoprotectant solution containing 50 mM MES (pH 6.3), 4 M sodium formate, 20 mM $MgCl_2$, 3 mM DTT, and 10% glycerol for about 1 s and then flash-frozen in liquid nitrogen. Native X-ray diffraction data were collected at station F1 of the Cornell High Energy Synchrotron Source (Ithaca, NY). X-ray data were collected at three different wavelengths at beamline X-8C of the National Synchrotron Light Source (Upton, NY) and at one additional wavelength using a laboratory X-ray source (Cu Kα radiation). The data were processed with DENZO/SCALEPACK (Otwinowski and Minor, 1997). Out of 14 potential selenium sites in two protein molecules, 11 were located by SOLVE (Terwilliger and Berendzen, 1999), and one more selenium site and two zinc sites were found by difference Fourier methods using the experimental phases. Two remaining selenium sites are located in the disordered N-terminal segment of the primase. Heavy atom refinement was performed with MLPHARE (Bailey, 1994), followed by density modification using DM (Cowtan and Main, 1996). The resulting electron density was of sufficient quality to model nearly all the primase residues by using O (Jones et al., 1991). Model refinement was carried out with CNS (Brunger et al., 1998), followed by the additional refinement cycles with REFMAC5 (Murshudov et al., 1997). The figures of the crystallographic model were prepared using MOLSCRIPT (Kraulis, 1991), Ribbons (Carson, 1997), and GRASP (Nicholls et al., 1991). The coordinates of T7 primase have been deposited in the Protein Data Bank (accession code 1NUI).

NMR Spectroscopy

Two dimensional ^{1}H-^{15}N HSQC spectra were collected with a Varian INOVA (500 MHz) spectrometer for samples containing 75 μM perdeuterated-^{15}N-labeled T7 primase in 200 mM HEPES (pH 7.5), 100 mM NaCl, 20 mM DTT, 1 mM EDTA, 0.1 mM PMSF, and 20 mM $MgCl_2$ in 90% H_2O/10% D_2O at 25°C. The addition of 0.2 mM DNA template (5′-GGGTCAA-3′) and each 1 mM ATP and CTP to the above solution eliminated or changed the positions of many peaks in the 2D HSQC spectrum, suggesting that a complex with the primase had formed. A slight precipitation appeared during the NMR experiment, and this problem was solved by substituting the nucleotides with a preformed RNA primer (0.4 mM each of 5′-ACCC-3′ and DNA template). The spectra of the ^{15}N-labeled ZBD were measured using 0.5 mM protein in the same buffer described above, but without the template and primer. All spectra were processed using NMRPipe (Delaglio et al., 1995) and analyzed with NMRView (Johnson and Blevins, 1994). ^{15}N T_1 and T_2 values of T7 primase were measured from the spectra recorded with eight different durations of the delay T: for T_1, T = 10, 40 120, 240, 480, 720, 960, and 1200 ms; for T_2, T = 10, 30, 50, 70, 90, 110, 130, and 150 ms (Farrow et al., 1994). Analyses of T_1 and T_2 values were carried out with the automated function of NMRView. Well-dispersed peaks corresponding to the ZBD and RPD were randomly picked, and the averaged values were calculated for the ZBD and RPD separately (see Supplemental Data at http://www.molecule.org/cgi/content/full/11/5/1349/DC1).

Modeling the Primase-DNA Complex

The structure of the RNA polymerase II complexed with DNA:RNA hybrid strands (PDB code 1T6H) (Gnatt et al., 2001) was superimposed on the crystallographic model of T7 primase. The highly con-

served residues E157, D207, and D209 of T7 primase were aligned with the corresponding residues D485, D481, and D483 of RNA polymerase II (chain A; rmsd = 1.9 Å for these side chains). The superimposed DNA:RNA heteroduplex from RNA Pol II was displayed on the structure of T7 primase, and the ZBD was then manually adjusted to interact with the priming site of the DNA template so that D31 and H33 close to 3′ C of the 5′-GTC-3′ priming site.

Acknowledgments

We thank Eric Toth for assistance with X-ray data collection and discussions, Luis Brieba for providing the purified RPD, JoonSoo Lee, Seung-Joo Lee, and David Frick for advice on primase activity assays, and Patrick O'Brien and Ying Li for critically reading the manuscript. We also thank the beamline staff of the National Synchrotron Light Source (Upton, NY) and the Cornell High Energy Synchrotron Source (Ithaca, NY) for assistance with X-ray data collection. This work was supported by grants from the National Institutes of Health (R01 GM55390 to T.E. and R01 GM54397 to C.C.R.) and the National Science Foundation (NSF MCB9816072 to G.W.) and by the resources of the Harvard/Armenise Structural Biology Center at Harvard Medical School. M.K. was supported by a fellowship from the Uehara Memorial Foundation. T.E.E. gratefully acknowledges support from the Hsien Wu and Daisy Yen Wu Professorship at Harvard Medical School.

Received: January 23, 2003
Revised: April 15, 2003
Accepted: May 8, 2003
Published: May 22, 2003

References

Aravind, L., Leipe, D.D., and Koonin, E.V. (1998). Toprim—a conserved catalytic domain in type IA and II topoisomerases, DnaG-type primases, OLD family nucleases and RecR proteins. Nucleic Acids Res. *26*, 4205–4213.

Augustin, M.A., Huber, R., and Kaiser, J.T. (2001). Crystal structure of a DNA-dependent RNA polymerase (DNA primase). Nat. Struct. Biol. *8*, 57–61.

Bailey, S. (1994). The CCP4 suite-programs for protein crystallography. Acta Crystallogr. *D50*, 760–763.

Benkovic, S.J., Valentine, A.M., and Salinas, F. (2001). Replisome-mediated DNA replication. Annu. Rev. Biochem. *70*, 181–208.

Berger, J.M., Gamblin, S.J., Harrison, S.C., and Wang, J.C. (1996). Structure and mechanism of DNA topoisomerase II. Nature *379*, 225–232.

Bernstein, J.A., and Richardson, C.C. (1988). A 7-kDa region of the bacteriophage T7 gene 4 protein is required for primase but not for helicase activity. Proc. Natl. Acad. Sci. USA *85*, 396–400.

Bird, L.E., Hakansson, K., Pan, H., and Wigley, D.B. (1997). Characterization and crystallization of the helicase domain of bacteriophage T7 gene 4 protein. Nucleic Acids Res. *25*, 2620–2626.

Bird, L.E., Pan, H., Soultanas, P., and Wigley, D.B. (2000). Mapping protein-protein interactions within a stable complex of DNA primase and DnaB helicase from *Bacillus stearothermophilus*. Biochemistry *39*, 171–182.

Brautigam, C.A., and Steitz, T.A. (1998). Structural and functional insights provided by crystal structures of DNA polymerases and their substrate complexes. Curr. Opin. Struct. Biol. *8*, 54–63.

Brunger, A.T., Adams, P.D., Clore, G.M., DeLano, W.L., Gros, P., Grosse-Kunstleve, R.W., Jiang, J.S., Kuszewski, J., Nilges, M., Pannu, N.S., et al. (1998). Crystallography & NMR system: a new software suite for macromolecular structure determination. Acta Crystallogr. D Biol. Crystallogr. *54*, 905–921.

Carson, M. (1997). Ribbons. In Methods in Enzymology, C.W. Carter, Jr., and R.M. Sweet, eds. (Orlando: Academic Press), pp. 493–505.

Chang, P., and Marians, K.J. (2000). Identification of a region of *Escherichia coli* DnaB required for functional interaction with DnaG at the replication fork. J. Biol. Chem. *275*, 26187–26195.

Chowdhury, K., Tabor, S., and Richardson, C.C. (2000). A unique loop in the DNA-binding crevice of bacteriophage T7 DNA polymerase influences primer utilization. Proc. Natl. Acad. Sci. USA *97*, 12469–12474.

Cowtan, K., and Main, P. (1996). Phase combination and cross validation in iterated density-modification calculation. Acta Crystallogr. *D52*, 43–48.

Delaglio, F., Grzesiek, S., Vuister, G.W., Zhu, G., Pfeifer, J., and Bax, A. (1995). NMRPipe: a multidimensional spectral processing system based on UNIX pipes. J. Biomol. NMR *6*, 277–293.

Doublie, S., and Ellenberger, T. (1998). The mechanism of action of T7 DNA polymerase. Curr. Opin. Struct. Biol. *8*, 704–712.

Dunn, J.J., and Studier, F.W. (1983). Complete nucleotide sequence of bacteriophage T7 DNA and the locations of T7 genetic elements. J. Mol. Biol. *166*, 477–535.

Egelman, H.H., Yu, X., Wild, R., Hingorani, M.M., and Patel, S.S. (1995). Bacteriophage T7 helicase/primase proteins form rings around single-stranded DNA that suggest a general structure for hexameric helicases. Proc. Natl. Acad. Sci. USA *92*, 3869–3873.

Farrow, N.A., Muhandiram, R., Singer, A.U., Pascal, S.M., Kay, C.M., Gish, G., Shoelson, S.E., Pawson, T., Forman-Kay, J.D., and Kay, L.E. (1994). Backbone dynamics of a free and phosphopeptide-complexed Src homology 2 domain studied by 15N NMR relaxation. Biochemistry *33*, 5984–6003.

Frick, D.N., and Richardson, C.C. (1999). Interaction of bacteriophage T7 gene 4 primase with its template recognition site. J. Biol. Chem. *274*, 35889–35898.

Frick, D.N., and Richardson, C.C. (2001). DNA primases. Annu. Rev. Biochem. *70*, 39–80.

Frick, D.N., Baradaran, K., and Richardson, C.C. (1998). An N-terminal fragment of the gene 4 helicase/primase of bacteriophage T7 retains primase activity in the absence of helicase activity. Proc. Natl. Acad. Sci. USA *95*, 7957–7962.

Fujiyama, A., Kohara, Y., and Okazaki, T. (1981). Initiation sites for discontinuous DNA synthesis of bacteriophage T7. Proc. Natl. Acad. Sci. USA *78*, 903–907.

Gnatt, A.L., Cramer, P., Fu, J., Bushnell, D.A., and Kornberg, R.D. (2001). Structural basis of transcription: an RNA polymerase II elongation complex at 3.3 Å resolution. Science *292*, 1876–1882.

Godson, G.N., Schoenich, J., Sun, W., and Mustaev, A.A. (2000). Identification of the magnesium ion binding site in the catalytic center of *Escherichia coli* primase by iron cleavage. Biochemistry *39*, 332–339.

Griep, M.A. (1995). Primase structure and function. Indian J. Biochem. Biophys. *32*, 171–178.

Guo, S., Tabor, S., and Richardson, C.C. (1999). The linker region between the helicase and primase domains of the bacteriophage T7 gene 4 protein is critical for hexamer formation. J. Biol. Chem. *274*, 30303–30309.

Holm, L., and Sander, C. (1993). Protein structure comparison by alignment of distance matrices. J. Mol. Biol. *233*, 123–138.

Ilyina, T.V., Gorbalenya, A.E., and Koonin, E.V. (1992). Organization and evolution of bacterial and bacteriophage primase-helicase systems. J. Mol. Evol. *34*, 351–357.

Johnson, B.A., and Blevins, R.A. (1994). NMRView: a computer program for the visualization and analysis of NMR data. J. Biomol. NMR *4*, 603–614.

Jones, T.A., Zou, J.Y., Cowan, S.W., and Kjeldgaard (1991). Improved methods for building protein models in electron density maps and the location of errors in these models. Acta Crystallogr. A *47 (Pt 2)*, 110–119.

Kato, M., Frick, D.N., Lee, J., Tabor, S., Richardson, C.C., and Ellenberger, T. (2001). A complex of the bacteriophage T7 primase-helicase and DNA polymerase directs primer utilization. J. Biol. Chem. *276*, 21809–21820.

Keck, J.L., and Berger, J.M. (2001). Primus inter pares (first among equals). Nat. Struct. Biol. *8*, 2–4.

Keck, J.L., Roche, D.D., Lynch, A.S., and Berger, J.M. (2000). Structure of the RNA polymerase domain of E. coli primase. Science *287*, 2482–2486.

Kraulis, P.J. (1991). MOLSCRIPT: a program to produce both detailed and schematic plots of protein structures. J. Appl. Crystallogr. *24*, 946–950.

Kusakabe, T., and Richardson, C.C. (1996). The role of the zinc motif in sequence recognition by DNA primases. J. Biol. Chem. *271*, 19563–19570.

Kusakabe, T., and Richardson, C.C. (1997). Gene 4 DNA primase of bacteriophage T7 mediates the annealing and extension of ribo-oligonucleotides at primase recognition sites. J. Biol. Chem. *272*, 12446–12453.

Kusakabe, T., Baradaran, K., Lee, J., and Richardson, C.C. (1998). Roles of the helicase and primase domain of the gene 4 protein of bacteriophage T7 in accessing the primase recognition site. EMBO J. *17*, 1542–1552.

Kusakabe, T., Hine, A.V., Hyberts, S.G., and Richardson, C.C. (1999). The Cys4 zinc finger of bacteriophage T7 primase in sequence-specific single-stranded DNA recognition. Proc. Natl. Acad. Sci. USA *96*, 4295–4300.

Lee, J., Chastain, P.D., Kusakabe, T., Griffith, J.D., and Richardson, C.C. (1998). Coordinated leading and lagging strand DNA synthesis on a minicircular template. Mol. Cell *1*, 1001–1010.

Lee, S.J., and Richardson, C.C. (2001). Essential lysine residues in the RNA polymerase domain of the gene 4 primase-helicase of bacteriophage T7. J. Biol. Chem. *276*, 49419–49426.

Lee, S.J., and Richardson, C.C. (2002). Interaction of adjacent primase domains within the hexameric gene 4 helicase-primase of bacteriophage T7. Proc. Natl. Acad. Sci. USA *99*, 12703–12708.

Lima, C.D., Wang, J.C., and Mondragon, A. (1994). Three-dimensional structure of the 67K N-terminal fragment of E. coli DNA topoisomerase I. Nature *367*, 138–146.

Marintcheva, B., and Weller, S.K. (2001). A tale of two HSV-1 helicases: roles of phage and animal virus helicases in DNA replication and recombination. Prog. Nucleic Acid Res. Mol. Biol. *70*, 77–118.

Matson, S.W., Tabor, S., and Richardson, C.C. (1983). The gene 4 protein of bacteriophage T7. Characterization of helicase activity. J. Biol. Chem. *258*, 14017–14024.

Mendelman, L.V., and Richardson, C.C. (1991). Requirements for primer synthesis by bacteriophage T7 63-kDa gene 4 protein. Roles of template sequence and T7 56-kDa gene 4 protein. J. Biol. Chem. *266*, 23240–23250.

Mendelman, L.V., Beauchamp, B.B., and Richardson, C.C. (1994). Requirement for a zinc motif for template recognition by the bacteriophage T7 primase. EMBO J. *13*, 3909–3916.

Mondragon, A., and DiGate, R. (1999). The structure of *Escherichia coli* DNA topoisomerase III. Struct. Fold. Des. *7*, 1373–1383.

Murshudov, G.N., Vagin, A.A., and Dodson, E.J. (1997). Refinement of macromolecular structures by the maximum-likelihood method. Acta Crystallogr. *D53*, 240–255.

Mustaev, A.A., and Godson, G.N. (1995). Studies of the functional topography of the catalytic center of *Escherichia coli* primase. J. Biol. Chem. *270*, 15711–15718.

Nicholls, A., Sharp, K.A., and Honig, B. (1991). Protein folding and association: insights from the interfacial and thermodynamic properties of hydrocarbons. Proteins *11*, 281–296.

Nichols, M.D., DeAngelis, K., Keck, J.L., and Berger, J.M. (1999). Structure and function of an archaeal topoisomerase VI subunit with homology to the meiotic recombination factor Spo11. EMBO J. *18*, 6177–6188.

Otwinowski, Z., and Minor, W. (1997). Processing of X-ray diffraction data collected in oscillation mode. In Methods in Enzymology, C.W. Carter, Jr., and R.M. Sweet, eds. (Orlando: Academic Press), pp. 307–326.

Pan, H., and Wigley, D.B. (2000). Structure of the zinc-binding domain of *Bacillus stearothermophilus* DNA primase. Struct. Fold. Des. *8*, 231–239.

Patel, S.S., Rosenberg, A.H., Studier, F.W., and Johnson, K.A. (1992). Large scale purification and biochemical characterization of T7 primase/helicase proteins. Evidence for homodimer and heterodimer formation. J. Biol. Chem. *267*, 15013–15021.

Podobnik, M., McInerney, P., O'Donnell, M., and Kuriyan, J. (2000). A TOPRIM domain in the crystal structure of the catalytic core of *Escherichia coli* primase confirms a structural link to DNA topoisomerases. J. Mol. Biol. *300*, 353–362.

Powers, L., and Griep, M.A. (1999). *Escherichia coli* primase zinc is sensitive to substrate and cofactor binding. Biochemistry *38*, 7413–7420.

Qian, X., Jeon, C., Yoon, H., Agarwal, K., and Weiss, M.A. (1993). Structure of a new nucleic-acid-binding motif in eukaryotic transcriptional elongation factor TFIIS. Nature *365*, 277–279.

Richardson, C.C. (1983). Bacteriophage T7: minimal requirements for the replication of a duplex DNA molecule. Cell *33*, 315–317.

Rosenberg, A.H., Griffin, K., Washington, M.T., Patel, S.S., and Studier, F.W. (1996). Selection, identification, and genetic analysis of random mutants in the cloned primase/helicase gene of bacteriophage T7. J. Biol. Chem. *271*, 26819–26824.

Sawaya, M.R., Guo, S., Tabor, S., Richardson, C.C., and Ellenberger, T. (1999). Crystal structure of the helicase domain from the replicative helicase-primase of bacteriophage T7. Cell *99*, 167–177.

Singleton, M.R., Sawaya, M.R., Ellenberger, T., and Wigley, D.B. (2000). Crystal structure of T7 gene 4 ring helicase indicates a mechanism for sequential hydrolysis of nucleotides. Cell *101*, 589–600.

Steitz, T.A. (1998). A mechanism for all polymerases. Nature *391*, 231–232.

Sun, W., Schoneich, J., and Godson, G.N. (1999). A mutant Escherichia coli primase defective in elongation of primer RNA chains. J. Bacteriol. *181*, 3761–3767.

Tabor, S., and Richardson, C.C. (1981). Template recognition sequence for RNA primer synthesis by gene 4 protein of bacteriophage T7. Proc. Natl. Acad. Sci. USA *78*, 205–209.

Terwilliger, T.C., and Berendzen, J. (1999). Automated MAD and MIR structure solution. Acta Crystallogr. D Biol. Crystallogr. *55*, 849–861.

Urlacher, T.M., and Griep, M.A. (1995). Magnesium acetate induces a conformational change in *Escherichia coli* primase. Biochemistry *34*, 16708–16714.

Valentine, A.M., Ishmael, F.T., Shier, V.K., and Benkovic, S.J. (2001). A zinc ribbon protein in DNA replication: primer synthesis and macromolecular interactions by the bacteriophage T4 primase. Biochemistry *40*, 15074–15085.

Van Duyne, G.D., Standaert, R.F., Karplus, P.A., Schreiber, S.L., and Clardy, J. (1993). Atomic structures of the human immunophilin FKBP-12 complexes with FK506 and rapamycin. J. Mol. Biol. *229*, 105–124.

VanLoock, M.S., Chen, Y.J., Yu, X., Patel, S.S., and Egelman, E.H. (2001). The primase active site is on the outside of the hexameric bacteriophage T7 gene 4 helicase-primase ring. J. Mol. Biol. *311*, 951–956.

Vassylyev, D.G., Sekine, S., Laptenko, O., Lee, J., Vassylyeva, M.N., Borukhov, S., and Yokoyama, S. (2002). Crystal structure of a bacterial RNA polymerase holoenzyme at 2.6 Å resolution. Nature *417*, 712–719.

von Hippel, P.H., and Jing, D.H. (2000). Structural biology. Bit players in the trombone orchestra. Science *287*, 2435–2436.

Yuzhakov, A., Kelman, Z., and O'Donnell, M. (1999). Trading places on DNA–a three-point switch underlies primer handoff from primase to the replicative DNA polymerase. Cell *96*, 153–163.

Ziegelin, G., Linderoth, N.A., Calendar, R., and Lanka, E. (1995). Domain structure of phage P4 alpha protein deduced by mutational analysis. J. Bacteriol. *177*, 4333–4341.

Accession Numbers

The model coordinates and structure factors for the T7 primase are deposited in the Protein Data Bank with the accession number 1NUI.